Springer

KSME

Journal of Mechanical Science and Technology 29 (10) (2015) 4473~4481
www.springerlink.com/content/1738-494x(Print)/1976-3824(Online)
DOI 10.1007/s12206-015-0946-8

The SGT-600 industrial twin-shaft gas turbine modeling for mechanical drive applications at the steady state conditions †

Hiva Rashidzadeh[1], Seyed Mostafa Hosseinalipour[2,*] and Alireza Mohammadzadeh[1]

[1]*Department of Mechanical and Aerospace Engineering, Science and research branch, Islamic Azad University, Tehran, Iran*
[2]*Department of Mechanical Engineering, Iran University of Science and Technology, Tehran, Iran*

(Manuscript Received September 30, 2014; Revised April 20, 2015; Accepted May 11, 2015)

Abstract

The industrial gas turbines which are in service for power generation and mechanical drive are operated in different environmental conditions. The changes in environmental conditions could affect the performance of different main subsystems and also overall performance of the engine. It is very crucial to have a good insight regarding the behavior of the engine under different inlet air conditions. This paper presents the SGT-600 twin-shaft gas turbine design and off-design model for mechanical drive applications. Also the integration of components and component matching of the gas turbine at base and part loads are studied. The characteristic curves of each component derived from three-dimensional numerical simulations, were validated with experimental data in a separate study. The results of simulation are presented at the part load and different ambient conditions are validated with test measurement data. The results show good agreement between the experimental data and analytic model.

Keywords: SGT-600 gas turbine; Zero dimensional models; Off design condition; Design point

1. Introduction

The gas turbines have an important role in different industrial fields such as gas compression stations, power generation and combined steam and power plants. Their usage has been increased specially in recent years because of considerable improvements which have been achieved in their operation and efficiency. The "heavy duty" gas turbines operate at the off-design conditions in the most of their operation time. It is possible to gain more details information about a gas turbine operation by developing steady state mathematical models. These models are usually used as a fast and dependable tool for different studies such as parametric and sensitivity analysis, improving the control philosophy of the system. This paper presents a part of results produced by a developed steady state model which has been conducted for the SGT-600 gas turbine. The developed model in this paper has the capability of analyzing the gas turbine behavior in both design and off-design conditions based on continuity and energy equations for different parts of the system. In this study, detailed and exact results of the effects of the different parameters on the gas turbine performance have been presented. These results have been generated in the steady state condition with considering the control philosophy of the gas turbine operation. The control philosophy of the SGT-600 gas turbine based on the real control logic correlations is considered in this paper. It is possible to change the control philosophy of the gas turbine such as TIT constant, TET constant and IGV constant, … which is applicable for the simple or combined cycle based on designer's point of view.

The steady state modeling of a gas turbine is focused on the engine operation on different loads as well as the diverse control philosophies. These types of mathematical models enable the designer to calculate the required heat flow, Inlet guide vane (IGV) position and the mass flow rates of the bleed valves at different fuel compositions and environmental conditions. Moreover, the overall operation status of the main components such as intake, air compressor, combustion chamber, turbines and exhaust could be derived. The analysis of the main components conditions provide a good insight for deriving the best control philosophy for a specific condition in order to have an optimized operation for all components. Most of the previous researches were focused only on the design point operation models. There are also some off-design models reported by the researchers. On 1975, NASA developed a model "DYNGEN" for analyzing the operation of turbofan and turbojet engines on both the design and off-design conditions [1]. Waters and his colleagues developed a model "EPRI-GATE" for performance analysis of power cycle

*Corresponding author. Tel.: +98 2177240492, Fax.: +98 2177240492
E-mail address: alipour@iust.ac.ir
† Recommended by Associate Editor Tong Seop Kim

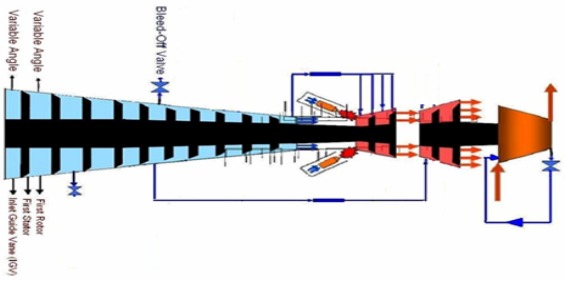

Fig. 1. Selected gas turbine schematic for mechanical drive application.

[2], which was later improved by Giglio via considering the effect of cooling process in the previous models [3]. El-Masri and his colleagues developed a more detailed model considering the blade cooling [4, 5]. El-Masri also developed some models based on the second thermodynamic law and cycle performance analysis with cooling which finally resulted in the GASCAN computer code [6-9]. Other zero dimensional models were developed for thermal analysis by Isamil and Bhinder in 1991 [10] as well as Zhu and Saravanamutto in 1992 [11].

Kim presented a mathematical model for both single and twin-shaft gas turbines with turbo-generator application [12]. Al-Hadman and Ebaid proposed a model for gas turbine engines under power generation application on 2005 [13]. More recently an off-design model for a Solar Centaur-40 gas turbine was suggested by Gobran [14].

2. Analytical modeling

This research is focused on SGT-600 gas turbine whose schematic view with mechanical drive application is shown in Fig. 1. As shown in this figure, the considered gas turbine is composed of a 10-stage air compressor with IGV at the inlet for higher performance at off-design conditions; meanwhile they also provide the required safe margin from the surge line of the compressor at speeds lower than the design speed. The bleed valves which are located after 2nd and 5th stages have an important role for controlling the safe margin of the air compressor. The positions of these valves are usually determined based on the shaft speed. Also the flow coefficients of these valves have a vital role in the simulation. These coefficients have been derived for different positions considering the different pressure on both sides of the valves as well as the risk of the choking in flow.

The outlet air from the compressor is introduced to an annular combustion chamber and mixes with the fuel which is directed to the burner from another path. The mixture is ignited and the temperature of the outlet gas is increased. The hot gas mixture is introduced to the first-vanes row of the turbine and then revolves the first-blades row of turbine. These rows are cooled with milder temperature air in order to prevent the blades from the risk of firing because of the high temperature. The SGT-600 gas turbine is a twin-shaft which consist a high pressure turbine for driving the air compressor and a low pressure one for driving a gas compressor working in a gas transmission line. A fraction of the compressor outlet stream is used to cool the vanes and blades of high pressure turbine. Also the first row vanes of the power turbine are cooled by the air which is extracted from the 5th stage of the air compressor. The rest of the rows do not require to be cooled because of the lower gas temperature in this region.

The agent air and flue gases are considered as ideal gases through all gas turbine components. The correlation used for calculating the thermodynamic properties of the mixtures are based on the Van Wylen [15]. Thermodynamic properties of the transmission natural gas were calculated using correlations provided in Refs. [16, 17].

A complete adiabatic combustion chamber process was considered for the combustion of the natural gas inside the engine combustor. The different selected parts and components of the engine were considered as separated control volumes which were related by the thermodynamic properties of the working fluid at their inlets and outlets. The mass and energy conservation equations were applied for all these control volumes and the overall model were constructed by integration of separate parts using matching roles between different components.

2.1 Design point modeling

An environment with 15°C temperature, 1atm absolute pressure and 60% relative humidity considered as the design point condition. The isentropic efficiency of the air compressor and turbine stages, the pressure loss of the combustion chamber and intake and exhaust, turbine inlet temperature, the inlet station gas temperature and pressure as well as the fuel, combustion efficiency, gas generator and power turbine speeds were considered as known input data for design point calculations. On the other hand, the coolant mass flow rates, power required for compressor and power generated from the high and low pressure turbines, fuel and air mass flow rates, air compressor pressure ratio and gas flow rate from the gas compressor are the main unknowns which can be calculated using the thermodynamic model. The cooling model is based on the El-Masri which is proposed for design point cooling of the turbine blades [9].

A computer code in FORTRAN language has been developed which was capable of calculating the thermodynamic properties at all sections of the gas turbine engine. The proposed model was used for studying the effects of any change in input parameters on the engine performance. The power and efficiency of overall engine were determined from Eqs. (1) and (2).

$$W_{net-cycle} = W_{turb} - W_{comp} \tag{1}$$

$$\eta_{th} = \frac{W_{net-cycle}}{\dot{m}_f LHV \eta_{cc}} \tag{2}$$

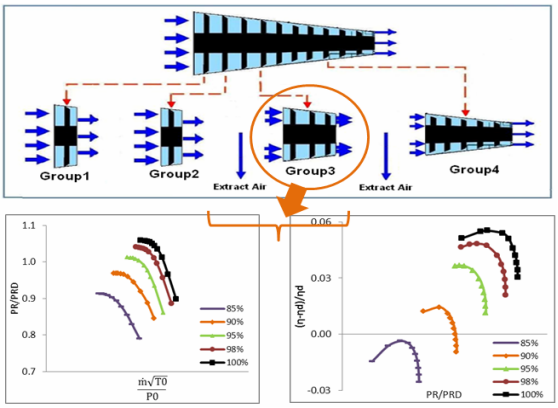

Fig. 2. Air compressor groups and compressor group 3 maps.

where W_{comp} and W_{turb} are compressor and turbine power respictively, $\dot{m}_f$ denotes fuel mass flow rate, LHV is the lower heating value of fuel, and η_{cc} is combustion efficiency.

The different parameters such as mass flow rate, pressure ratio, polytropic efficiency were calculated from design point results and used for producing dimensionless characteristic curves of the air compressor, turbines and calculating pressure loss of air intake and exhaust and also as first initial guesses at off-design conditions.

2.2 Off- design modeling

2.2.1 Air intake and exhaust

The only needed parameters of the air intake and exhaust are the pressure loss of working fluid when passing these two components. These amounts were calculated by Eq. (3) for off-design conditions using the calculated values for design point condition [18].

$$\left(\frac{\Delta P}{P_0}\right)=\left(\frac{\Delta P}{P_0}\right)_D \times \left[\frac{\left(\frac{\dot{m}\sqrt{T_0}}{P_0}\right)}{\left(\frac{\dot{m}\sqrt{T_0}}{P_0}\right)_D}\right]^2 \quad (3)$$

where T_0, P_0 and $\dot{m}$ are stagnation temperature, stagnation pressure and air mass flow rate respectively, and ΔP denotes the pressure loss. Subscript D denoted the design point.

2.2.2 Air compressor

In the off-design model, the compressor was divided into four different groups as indicated in Fig. 2. The performance maps of these groups were produced using full three-dimensional (3-D) numerical simulations and the necessary figures for different conditions were selected from these curves and were feed into the off-design model of the compressor group 3 maps are shown at Fig. 2.

The 3D modeling of the compressor has been done accurately. Great efforts have been done for considering the details of the geometries of the compressor. The numerical simulations were conducted using CFX-Ansys software and the SST K-ω turbulence model. Fig. 3 indicates a brief procedure of the simulation. For validation of the generated curves, the available data for the compressor inlet and outlet and rotational speed is used from the experiment data of the Test Rig.

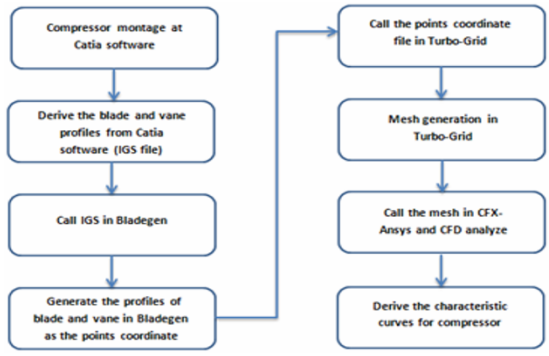

Fig. 3. Compressor 3D numerical simulation process.

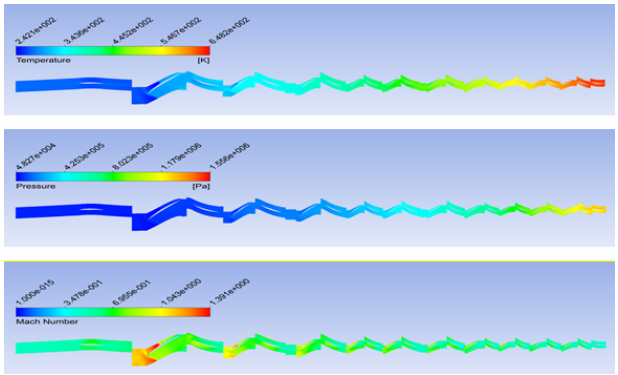

Fig. 4. Distribution of temperature, pressure and relative Mach number at 50% span at 100% GG speed.

Fig. 4 presents the temperature, pressure and relative Mach number contours at 50% span at 100% GG (Gas generator) speed for all rows of compressor. It is observed that the temperature and pressure are increasing at the final rows of the compressor. However, the relative Mach number of the first stage is high because of the transonic flow field.

2.2.3 Combustion chamber

The simple and robust Dry low emission (DLE) combustor is based on an aero-derivative film-cooled concept. The selective combustor chamber is an annular type with 18 burners. Effective parameters on combustion chamber performance are pressure loss and combustion efficiency. Combustion efficiency is defined as the ratio of the actual fuel-air ratio for given temperature difference between combustor inlet and exit to theoretical fuel-air ratio [18]. The combustion efficiency acts as an input. This amount has been considered equal to 0.99 in our study and the necessary amounts in the off-design conditions came from combustor characteristic curve which is produced by a full 3-D numerical simulation.

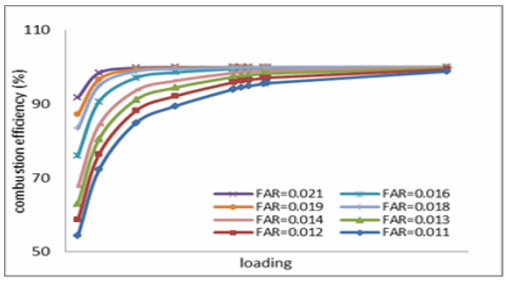

Fig. 5. Characteristic curve of combustion efficiency versus loading parameter.

Fig. 5 presents the combustion efficiency as a function of loading parameter which is defined by the following expression:

$$Loading = \frac{P^{1.75} \times 0.222 \times e^{\frac{T}{300}}}{\dot{m}}. \quad (4)$$

The combustor pressure loss is calculated by the 3-D numerical simulation for on and off-design conditions using:

$$\Delta P_{total} = 0.0004\left(\frac{\dot{m}\sqrt{T_0}}{P_0}\right)^2 + 0.0076\left(\frac{\dot{m}\sqrt{T_0}}{P_0}\right). \quad (5)$$

A geometric model (consisting of 30 million elements) is generated for 3D stream flow from the compressor outlet to the combustion chamber outlet. The model is included the diffuser, annulus, burner, burner metal and coating. The governing equations for fluid flow, heat transfer and combustion are fully solved using a conjugate technique in order to consider the most important physics involved in the problem. The standard and realizable K-ε turbulence model was used in the simulations. The boundary conditions for the combustion chamber are as the inlet total pressure and temperature as well as the outlet static pressure. Meanwhile, the existing experimental correlations are used for combustion efficiency calculation [19]. Finally, the existing correlation of the Refs. [20, 21] are used for the pressure loss validation.

The Velocity and pressure contours of combustion chamber are shown in the Figs. 6 and 7. The maximum velocity occurs at the first of the diffuser and is about 210 m/s. So, regarding to the role of the diffuser in increasing the static pressure by decreasing the velocity, the velocity decreases from 210 m/s to 105 m/s at the inlet section of the burner. The pressure at the downstream of the inner annulus is lower than the outer annulus, so the outlet mass flow rate and stream velocity are higher at the inner annulus compared to the outer one. For instance, the maximum velocity at the inner and outer annulus is about 80 m/s and 30 m/s, respectively.

2.2.4 High pressure and low pressure turbine

In order to gain the most appropriate information for the gas path, full 3-D simulations (the same as compressor method)

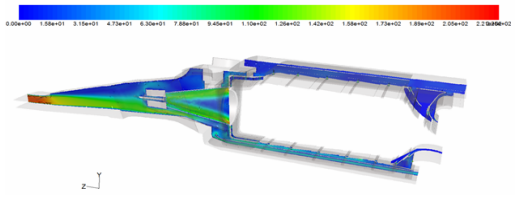

Fig. 6. Velocity distribution contour of combustion chamber.

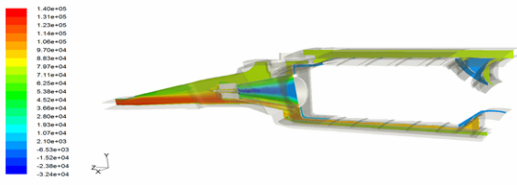

Fig. 7. Pressure distribution contour of combustion chamber.

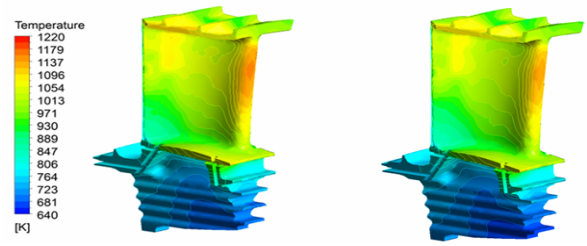

100% load 90% load

Fig. 8. The rotor blade temperature distribution at 100% and 90% load.

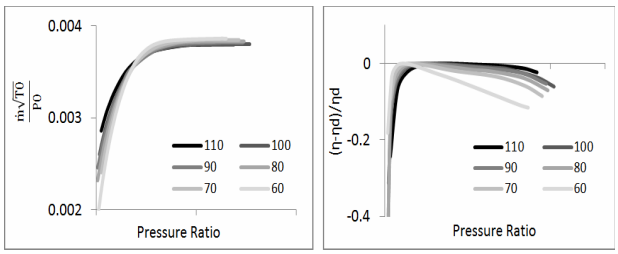

Fig. 9. Turbine stage 1 map.

have been conducted and the individual maps for all the stages are derived. The Contour of rotor blade temperature for first stage of GG at 100%, 90% load is shown in Fig. 8. It can be seen that at the root of the blade, the metal temperature is close to the coolant temperature and maximum temperature occurs at the leading edge.

Fig. 9 presents the stage 1 map for the uncooled situation. Also in order to consider the effects of swirl through the flow path between GG and Power turbine (PT), the speed of GG was fixed for different PT rotating speeds. This procedure was conducted for producing the maps of 3 and 4 stages.

2.2.5 Cooling model

In the presented study the blade cooling model of El-Masri was used, in which the blade temperature is considered as an input and the actual stage by stage expansion replaced by a continuous expansion process. The cooling process in each

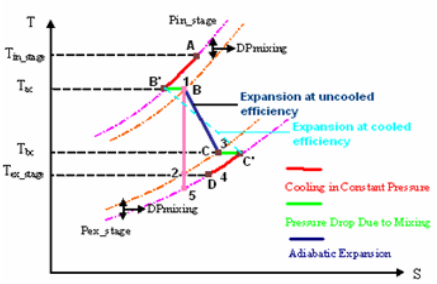

Fig. 10. Thermodynamic states of the stage model [9].

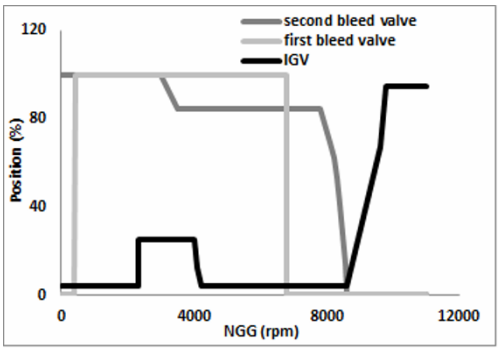

Fig. 11. IGV and bleed valves position versus gas generator speed.

stage is divided into 5 different steps. In the first step, a constant pressure cooling is considered (A-B' in Fig. 10) which presents the mixing of coolant with main flow inside the stator. The second step is considered as an isothermal pressure loss process which is due to mixing of coolant and main flow (B'-B in Fig. 10). The third step is an adiabatic expansion process inside the rotor. An isothermal pressure loss and a constant-pressure temperature drop inside the rotor are the two last steps; respectively [9].

2.2.6 Gas compressor

A seven stage centrifugal gas compressor is derived by the power turbine. The performance of this compressor has been considered as a part of proposed model. 3-D numerical simulations have been conducted in order to produce the compressor maps.

2.2.7 Control philosophy

As the control philosophy has a very crucial effect on the engine performance. There are different control philosophies for controlling the off-design engine performance for instance the constant turbine inlet temperature, constant turbine exhaust temperature and etc. The governor which is the main component and controls the engine operation determines the actuator position of the fuel valves, IGV and bleed valves.

In this study, the real logic control of the SGT-600 has been applied to the model. Thus, for predicting the fuel mass flow rate at the base load, turbine exhaust temperature set point (T_{7sp}) is calculated from the following equations. T_{7sp} is limited between [450, 580].

$$t_{3new} = \left(0.902T_{2av} - 0.0010187T_{2av}^2 + 366.24\right) \tag{6}$$

$$t_{3dev} = T_{3av} - t_{3new} \tag{7}$$

$$T_{7base} = 2.3036\times10^{-6}\times NPT^2 - 3.6553\times10^{-2} \times NPT + 144.8 + 12.05\left(\frac{P_{3av}}{P_{7av}}\right)^2 - 0.25\left(\frac{P_{3av}}{P_{7av}}\right)^3 - 198.75\left(\frac{P_{3av}}{P_{7av}}\right) + 1649.1 - \max\left(\frac{t_{3dev}}{2}, -5\right) \tag{8}$$

$$T_{7sp} = \begin{cases} T_{7base} + 33 & Peakload(\max = 580) \\ T_{7base} & Baseload(\max = 560) \end{cases} \tag{9}$$

where T_{2av} is average temperature at compressor inlet, P_{3av} is average pressure at compressor exit, P_{7av} is average pressure at turbine exit, and NPT denotes the power turbine shaft speed.

Meanwhile, the logic control of the inlet guide vane and bleed valves are applied to the model (Fig. 11).

In order to consider the effect of geometry on the performance analysis, the characteristics curves of the compressor, combustion chamber and turbine stages have been produced using 3D CFD simulations. As the IGV and BV positions and T_{7sp} are considered in the presented model it would be possible to analyze the gas turbine performance by changing the SGT-600 gas turbine control logic.

2.2.8 Gas turbine component matching

The operation point of any component is determined using off-design performance via component matching procedure. This try and error procedure starts from a couple of initial guesses for 17 parameters including 4 pressure ratios of 4 compressor groups, 4 pressure ratios of 4 turbine stages, 5 cooling mass flow rates, two rotational speeds of gas generator and power turbine, fuel mass flow rate and intake pressure loss and ends up to the best operation point determination. The matching equations include mass balance between the components, energy balance between the high pressure turbine and compressor as well as between the power turbine and gas compressor and finally reaching to a constant temperature equal to what the control philosophy dictates.

All the components of gas turbine modeled separately and the appropriate equations for these components are solved together in order to develop a complete off-design model. The unknown parameters such as coolant and bleed valves mass flow rates, turbine and compressor pressure ratios, two rotational speeds and fuel mass flow rate are determined using the Newton Raphson solver. The schematic view of the component matching is shown in Fig. 12. As shown in the figure, the characteristic curves are applied to the model as known input data. As mentioned previously, these characteristics curves are derived from a 3-D numerical simulation.

Fig. 13 depicts the solution algorithm used to determine the off-design conditions for the SGT-600 gas turbine with mechanical drive applications.

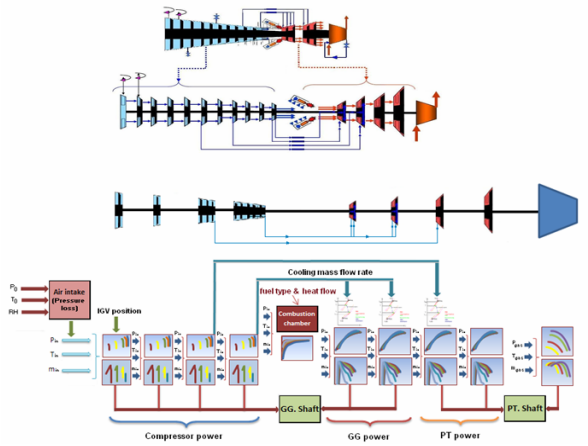

Fig. 12. Schematic view of component matching.

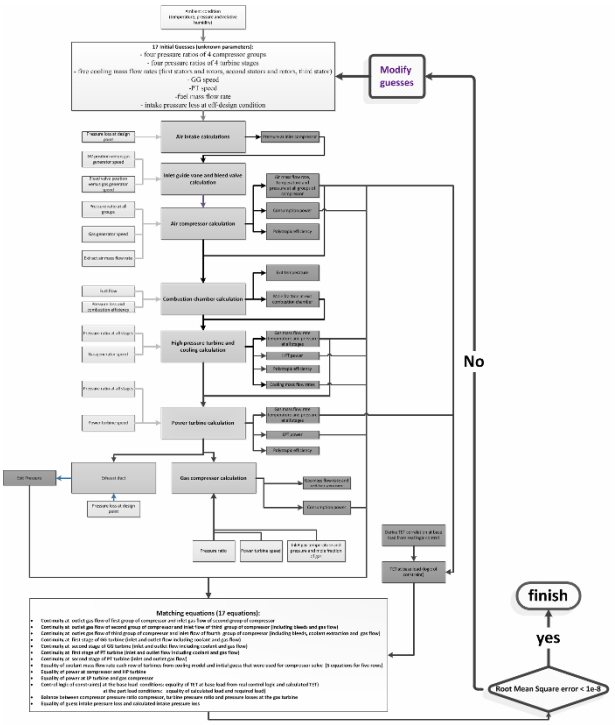

Fig. 13. Off-Design solution flowchart for the SGT-600 gas turbi-ne with mechanical drive application.

3. Simulation results

Fig. 14 depicts the variation of some important SGT-600 gas turbine performance parameters as a function of gas turbine load and also the operating points on compressor map during loading process. In all performed simulations the pure methane with 50037 kJ/kg lower heating value was considered as the fuel. An increase in load demand from the transportation line causes GG and PT speed up which will cause an increase in compressor air mass flow rate and compressor pressure ratio will occur. The power turbine will need more fuel in order to compensate the higher load demand which will produce higher TIT and TET. As the power change rate will

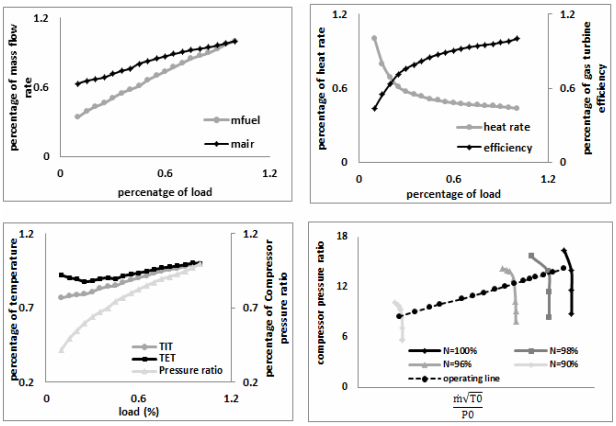

Fig. 14. Operational parameters variation against load at ISO conditions[1] (non dimensional).

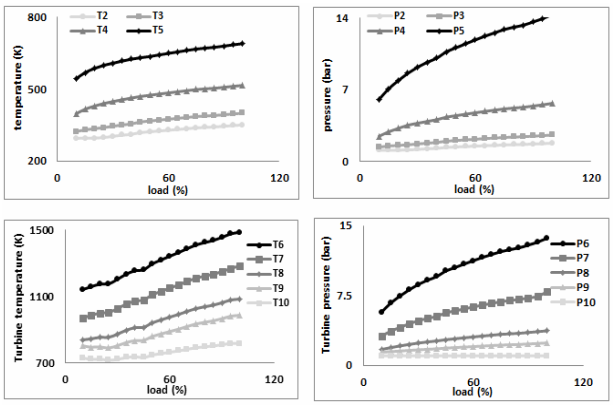

Fig. 15. Compressor and turbine temperatures and pressures vs load.

be greater than the heat release rate therefore an increase in heat rate and a decrease in thermal efficiency will happen when load decreases.

Fig. 15 present the compressor groups and turbine stages temperatures and pressures against the load; respectively. It is observed that all temperatures and pressures increase with increasing the load.

The effects of ambient air temperature and pressure on the output power and engine efficiency are presented as a function of load in Fig. 16. Increases in inlet air temperature or height from see level causes a lower air density and lower mass flow rate through compressor. This will decrease the gas turbine output power.

The fuel characteristic affects the gas turbine performance, majorly. Fig. 17 depicts the effects of the gasoil fuel (42680 kJ/kg LHV) and methane fuel (50037 kJ/kg LHV) on the SGT-600 output power and thermal efficiency. The higher fuel LHV causes lower fuel mass flow rate. This will increase the gas turbine thermal efficiency and output power.

4. The validation of developed steady state model

The model validation has been performed for design and

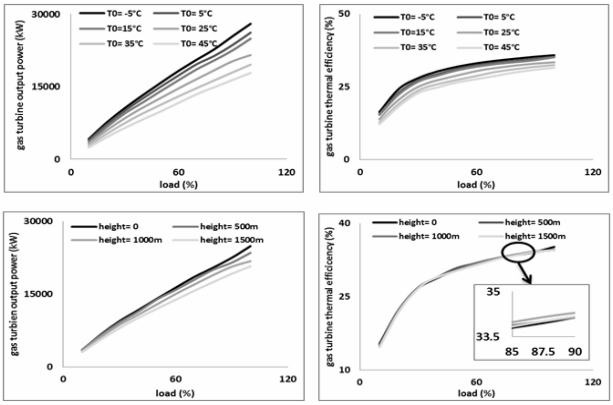

(a) Output power variation (b) Gas turbine efficiency variation

Fig. 16. The variation versus load change at different ambient temperatures and pressures.

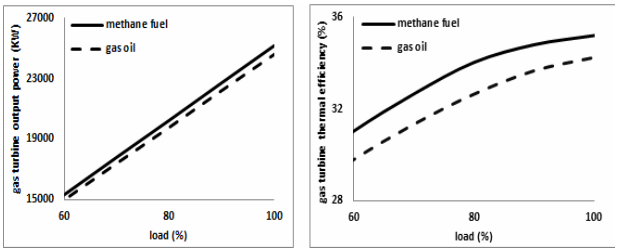

Fig. 17. Comparison between effects of methane fuel and gas oil on the SGT-600 performance at ISO condition.

some off-design points. The available experimental data for power generation applications which has been run using gas oil with 42680 KJ/kg lower heating value during the test in two steady state operation point were used in the validation procedure.

A pseudo infinity power distribution grid was assumed in order to justify a constant frequency behavior in the generator model. This allows the considering constant power turbine speed at 7700 rpm for all environmental regions and load conditions. The main difference between the results of MD and PG applications are mainly due to GG and PT speeds and fuel mass flow rate .The results of GG and PT speeds are presented as a function of load in Fig. 18.

The validation procedure was done in two steps. In the first step, the model results were compared with available experiment data, in base load (100% load) and 75% part load which were performed for the gas turbine with electric generator in the test hall. In the second step, the model simulation results were validated by some correlations which have been presented by the engine manufacturer reported in Ref. [22].

4.1 First step validation

The gas turbine power generation system has been tested in different ambient temperatures at 1060 meters above sea level. The available test results for ambient temperature equal to 11°C were used for validation of our proposed model. The

Table 1. Comparison between gas turbine operational parameters with test stand results at 100% load.

Gas turbine parameters	Test results	Simulation results	Error (%)
Output power (KW)	20330	20158	0.85
Gas generator speed (rpm)	9808	9801	0.07
Power turbine speed (rpm)	7726	7726	0.00
Air compressor exit pressure (bar)	12.70	12.58	0.95
TET (K)	546.8	540.5	1.16
Heat flow (MJ/sec)	61.75	61.01	1.21

Table 2. Comparison between gas turbine operational parameters with test stand results at 100% load.

Gas turbine parameters	Test results	Simulation results	Error (%)
Output power (KW)	15010	14865	0.97
Gas generator speed (rpm)	9370	9499	1.36
Power turbine speed (rpm)	7722	7722	0.00
Air compressor exit pressure (bar)	11.00	10.84	1.47
TET (K)	482.2	490.25	1.64
Heat flow (MJ/sec)	48.76	49.72	1.93

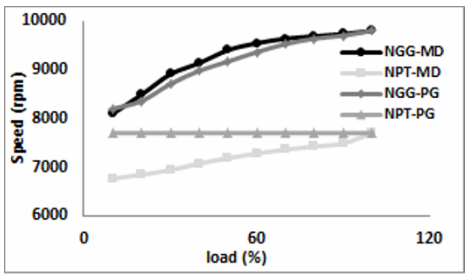

Fig. 18. Comparison between GG and PT speeds against the load for MD and PG applications of SGT-600.

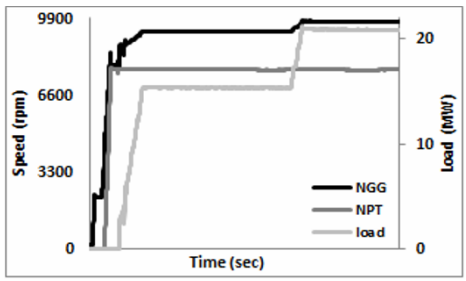

Fig. 19. Experiment data for selective gas turbine.

experimental data are depicted in Fig. 19 for time dependent engine operation up to the final steady state operation points at 75% and 100% loads.

The model simulation results are compared with aforementioned data in Tables 1 and 2. The results show a very good agreement between the model and test data's. The maximum

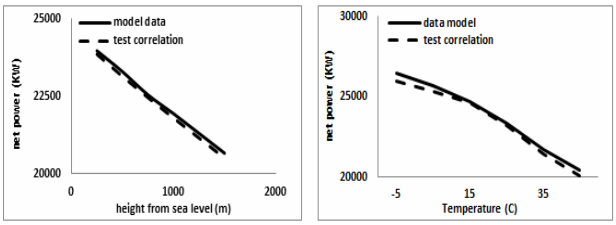

(a) At 15°C ambient temperature (b) At 1.01325bar ambient pressure

Fig. 20. Comparison between output power variation vs. ambient temperature and pressure variation.

error happens in predicting TET and heat flow which can be due to the difference between fuel composition in test and what has been used in the simulation.

4.2 Second step validation

In this step, the developed model has been run for some off-design points and the results were compared with what have been reported in the available documents provided by the engine manufacturer. The effect of some important operational parameters such as ambient pressure on net output power were studied and compared with calculated figures using the following correlation (Fig. 20) [22].

$$P_{sh-c} = \left(P_{sh-meas} + P_{loss-gear} + P_{loss-gen}\right) K_{P-T_0} K_{P-RH} K_{P-dpin} K_{P-dpout} K_{P-TIT} K_{P-f} \frac{P_{0ref}}{P_{0meas}} \quad (10)$$

where $K_{P\text{-}T0}$, $K_{P\text{-}RH}$, $K_{P\text{-}dpin}$, $K_{P\text{-}dpout}$, $K_{P\text{-}TIT}$ and $K_{P\text{-}f}$ are power output correction factor for inlet temperature, relative humidity, inlet pressure loss, outlet pressure loss, turbine inlet temperature and fuel, respectively. $P_{sh\text{-}c}$ denotes the corrected shaft power, $P_{sh\text{-}meas}$ is power output measured at generator, $P_{loss\text{-}gear}$ and $P_{loss\text{-}gen}$ are gear loss and generator loss respectively. P_{0ref} and P_{0meas} denote reference and measured ambient air pressures.

Again a very good agreement exists which shows the high accuracy of the proposed model in this study. The results show a maximum error equal to 1.01% in predicted net output power.

5. Conclusions

A mathematical model based on thermodynamic relations for the SGT-600 industrial gas turbine presented in this paper. The model was used to simulate the steady state behavior of gas turbine for mechanical drive application to study the effects of different parameters such as ambient conditions and loads. The three-dimensional flow effects were introduced in the model by application of characteristic curves of main subsystems such as air compressor, combustion chamber, HP (High pressure) turbine, LP (Low pressure) turbine and gas compressor. These curves were produced using 3-D CFD techniques in a separate study. The code is completely capable of predicting the gas turbine performance both in design and off-design conditions. The effects of inlet air conditions on the engine behavior were studied. The flow properties and gas turbine efficiency and output power at different loads were reported. The model results were compared with some available experimental data and correlation provided by the gas turbine manufacturer in order to show the high accuracy of the presented model. The model can be adapted for any single and twin-shaft industrial gas turbine using appropriate characteristic curves for each separate engine. One of the main advantages of the proposed model is its ability to consider the effects of geometrical and control parameters on the engine performance.

Acknowledgment

We would like to thank Mr. Hiva Khaledi and Mr. Behnam Rezaei for their most support and encouragement and unconditional guidance.

Nomenclature

CFD	: Computational fluid dynamic
IGV	: Inlet guide vane
mair	: Air mass flow rate (kg/sec)
mfuel	: Fuel mass flow rate (kg/sec)
MD	: Mechanical drive
MW	: Mega watt
N	: Speed (rpm)
NGG	: Gas generator speed (rpm)
NPT	: Power turbine speed (rpm)
PG	: Power Generation
PR	: Pressure ratio
T0	: Ambient temperature (ºC)
T	: Temperature (K)
TIT	: Turbine inlet temperature (K), T6
TET	: Turbine exit temperature (K), T10

Subscripts

2	: Compressor group 1 exit
3	: Compressor group 2 exit
4	: Compressor group 3 exit
5	: Compressor group 4 exit
6	: Turbine stage 1 inlet
7	: Turbine stage 2 inlet
8	: Turbine stage 3 inlet
9	: Turbine stage 4 inlet
10	: Turbine stage 4 exit

References

[1] J. Sellers and C. Daniele, DYNGEN-A program for calculat-

ing steady state and transient performance of turbojet and turbofan engines, *ASME Paper,* No. 83-GT-104 (1975).

[2] M. Waters and Associates Inc., Gas turbine evaluation (GATE) computer program, thermodynamic cycles, methods and sample programs, *EPRI Report AP-2871-CCM* (1983).

[3] R. S. Giglio, A thermodynamic performance analysis of a combined cycle engine, *M.S. Thesis*, Dept. of Mechanical Engineering, M.I.T. (1986).

[4] M. A. El-Masri, Y. Kobayashi and J. F. Louis, A general performance model for open-loop water cooled gas turbine, *ASME Paper*, No. 82-GT-212.

[5] J. F. Louis, K. Hiraoka and M. A. El-Masri, A comparative study of different means of turbine cooling on gas turbine performance, ASME Paper No. 83-GT-180, *Int. J. Turbo and Jet Eng*, 123-137.

[6] M. A. El-Masri, On thermodynamic of gas turbine cycles-Part1: Second law analysis of combined cycles, *ASME Journal of Engineering for Gas Turbine and Power*, 107 (1985) 880-889.

[7] M. A. El-Masri, On thermodynamic of gas turbine cycles-Part2: A model for expansion in cooled turbines, *ASME Journal of Engineering for Gas Turbine and Power*, 108 (1986) 151-159.

[8] M. A. El-Masri, On thermodynamic of gas turbine cycles-Part3: Thermodynamic potential and limitation of cooled reheat gas turbine combined cycles, *ASME Journal of Engineering for Gas Turbine and Power*, 108 (1986) 160-170.

[9] M. A. El-Masri, GASCAN-An interactive code for thermal analysis of gas turbine systems, *Journal of Eng. Gas Turbines Power*, 110 (1988).

[10] I. H. Ismail and F. S. Bhinder, Simulation of air craft gas turbine engines, *ASME Journal of Engineering for Gas Turbines and Power*, 113 (1991) 95-99.

[11] P. Zhu and H. I. H. Saravanamuttoo, Simulation of an advanced twin spool industrial gas turbine and power, *Journal of Engineering for Gas Turbine and Power*, 114 (1992) 180-186.

[12] J. H. Kim and T. S. Kim, Comparative analysis of off-design performance characteristics of single and two-shaft industrial gas turbines, *ASME*, 125 (2003).

[13] Q. Z. Al-Hamdan and M. S. Y. Ebaid, Modeling and simulation of a gas turbine engine for power generation**,** *J. Eng. Gas Turbines Power* (2005) 302-311.

[14] M. H. Gobran, Off-design performance of solar Centaur-40 gas turbine engine using Simulink, *Ain Shams Engineering Journal*, 4 (2013).

[15] G. VanWylen, C. Borgnakke and R. E. Sonntag, *Fundamentals of classical thermodynamics*, 5th Edition, John Wiley & Sons (1998).

[16] R. H. Aungier, A fast, accurate real gas equation of state for fluid dynamic analysis applications, *Journal of Fluid Eng.* (1995) 277-281.

[17] D. Green and R. Perry, *Perry's chemical engineering handbook*, 8th Edition, McGraw-Hill (2007).

[18] H. Cohen, H., G. F. C. Rogers and H. I. H. Saravanamuttoo, H. I. H. and P. Straznicky, *Gas turbine theory*, Pearson Education Limited (2009).

[19] H. Lefebvre and D. R. Ballal, *Gas turbine combustion: alternative fuels and emissions*, Taylor and Francis, Boca Raton, London, New York (2010).

[20] H. Mongia, S. A. Ahmed and H. C. Mongia, *An experimental investigation of gas jets in confined swirling air flow*, NASA, Washington, United states (1984).

[21] C. Duwig, L. Fuchs, A. Lacarelle, M. Beutke and C. O. Paschereit, Study of the vortex breakdown in a conical swirler using LDV, LES and POD, *ASME Turbo Expo: Power for Land, Sea, and Air*, Montreal, Canada (2007) 1-10.

[22] H. Waldfelt, N. Lennart and Y. Sedagati, *Test procedure mechanical running test*, Test rig in Iran, Ray: SIEMENS (2008) RT GRP 50/08.

Seyed Mostafa Hosseinalipour is currently an Associate Professor in the Department of Mechanical Engineering at Iran University of Science and Technology, Tehran, Iran. He earned his doctorate in Mechanical Engineering from McGill University, Montreal, Canada in 1996. His research interests include Optimization and design of energy consuming and energy conversion systems, HVAC and solar energy systems, CFD and parallel processing and turbomachinery. He has published over 100 articles in the peer-reviewed international journals and conference proceedings, and has delivered over 70 lectures in the international conferences.